

The Crystal Structure of Tl- β -Alumina

TOSHIKO KODAMA AND GIICHI MUTO

*The Institute of Industrial Science, The University of Tokyo, 22-1,
Roppongi 7-chome, Minato-ku, Tokyo 106*

Received June 18, 1975; in revised form August 28, 1975

The crystal structure of $\text{Tl}_2\text{O} \cdot 11\text{Al}_2\text{O}_3$ has been determined from three-dimensional X-ray data. The compound forms hexagonal crystals with $a = 5.598$, $c = 22.93$ Å, and $Z = 1$ in space group $P6_3/mmc$. The structure has been refined by least-squares methods with anisotropic temperature factors to an R value of 0.063 for 351 independent reflections collected by diffractometry. The crystal is composed of alternate stackings of the spinel block and the ion-conducting layer, both of which are linked together by the covalently bonded corner-sharing $\text{O}_3\text{Al}-\text{O}-\text{AlO}_3$ tetrahedra along the c -axis. The occupational percentages of the mobile ion were determined from the Fourier synthesis and compared with those of Ag- and Na- β -alumina.

Introduction

Superionic conductors have very high ionic conductivities comparable to those of conventional electrolyte solutions or molten salts. Accordingly, they are widely used in fuel cells (1, 2), transducer elements (3, 4), or as ion selective electrodes, etc (5-7).

In most ionic compounds, ionic conductivity is appreciable only at elevated temperatures in the solid state, and it arises from the thermal agitation of current-carrying defects created thermally in the crystal lattice (8-11). It is very interesting in view of the structural chemistry that many stable lattice defects exist in superionic conductors and the mobile ions can move easily between them (12-14).

Nonstoichiometric β -alumina compounds with the general formula, $M_2\text{O} \cdot 11\text{Al}_2\text{O}_3$, where M is Na, Ag, Li, K, Rb, or Tl, have high ionic conductivity in two-dimensions over a wide temperature range (15, 16) and the mobile ions can be exchanged with others with immersion in molten salts (17). The crystal structure of Na- and Ag- β -alumina was studied by Peters *et al.* (18) and Roth (19), respectively, and was discussed in relation to

their ionic conductivity. Tl- β -alumina has the largest lattice constant c among all of the β -alumina compounds due to the interlayer interactions. Moreover, the thallium ion is monovalent with electronic structure s^2p^1 in the outermost electronic shell because of the inert pair effect. The X-ray crystal structure analysis of Tl- β -alumina was undertaken to investigate the distribution of the conduction ions, and to clarify the atomic arrangement around the conduction ions.

Experimental

Samples of Tl- β -alumina were prepared from crystals of Na- β -alumina by the ion exchange technique (17). Crystals of Na- β -alumina were kindly supplied by Dr. Atuo Imai and Dr. Mituo Harata of Toshiba Research and Development Center of Tokyo Shibaura Electric Co. Crystals of Na- β -alumina in weight from 0.3661 to 1.8041×10^{-2} g were immersed in a lot of pure thallium nitrate at a temperature slightly above the melting point (mp, 206°C). Every 24 hr they were drawn up, washed with lukewarm water, weighed piece by piece on a microbalance, and immersed in a fresh batch of

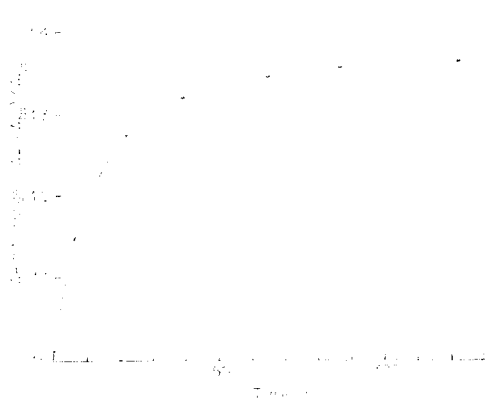


FIG. 1. Weight change versus immersion time of one of the pieces of TI- β -alumina (weight, 0.018 g; crystal size, 2.2×5.8 mm in the c -plane) in thallium nitrate molten solution.

fused thallium nitrate. The change of weight with immersion time of one of the pieces is shown in Fig. 1. During the last treatment, crystals were immersed continuously for 50 hr and were washed with water for only 30 sec in order to minimize the replacement of thallium ion by hydrogen or hydronium ions. The total immersion time was 138 hr.

Crystals of TI- β -alumina are colorless and transparent, and cleave easily to thin plates perpendicular to the c -axis. But the cutting of a crystal into a suitable shape was extremely difficult because of the hardness. They are hexagonal and have the Laue symmetry $6/mmm$. Systematically absent were hhl for $l = \text{odd}$. Lattice parameters were refined by a least-squares procedure using twenty-five 2θ values measured on a diffractometer. The space group $P6_3/mmc$ was assumed since the lattice parameters and the intensity distribution were similar to those of Na- and Ag- β -alumina, and was shown to be correct at the later stage of the structural refinement. The crystal density was determined by floating a crystal in thallium formate-water mixture. The crystal data are: hexagonal, space group $P6_3/mmc$; $a = 5.598 \pm 0.001$ Å; $c = 22.93 \pm 0.01$ Å; $V = 622.3 \pm 0.1$ Å³; $D_x = 4.49$ g·cm⁻³; $D_m = 4.2 \pm 0.2$ g·cm⁻³; and $\mu = 188$ cm⁻¹ for MoK α . (The crystal density calculated from the molecular composition which was determined at the last stage of the

structure refinement by the X-ray diffraction method was also shown in this table.)

One unit of the general formula, $\text{TI}_2\text{O} \cdot 11\text{Al}_2\text{O}_3$, was verified to be contained in a unit cell by the density measurement. The specimen with dimensions $0.05 \times 0.05 \times 0.03$ mm, being satisfied with the condition $\mu R \leq 1.0$, was used for the intensity measurement. Data were collected on a Rigaku Denki computer-controlled four-circle diffractometer using monochromated MoK α radiation with a graphite single crystal and a scintillation counter detector. Reflections hkl , $h \geq k \geq 0$ and $l \geq 0$, were measured over the section of the reciprocal lattice where the intensity of equivalent reflections changed most gradually from the nearest one to the next. Integrated intensities were measured by the θ - 2θ scan technique to a maximum 2θ of 100° . A scan range of ω for each reflection was calculated by the formula $\Delta\omega = 0.9^\circ + 0.5^\circ \times \tan \theta$. Attenuators were automatically inserted when the maximum counting rate exceeded 5500 cps. Three standard reflections, (008), (220), and (060), were measured every 50 reflections during the data collection. They showed non-systematic drifts (their standard deviations, 0.8, 1.0, and 1.4%, respectively) during the experiment. Reflections whose intensities were greater than two times their standard deviations were collected. The 351 independent reflections were collected and were corrected for background, Lorentz-polarization factors, but corrections for absorption, extinction, and anomalous dispersion were not applied.

Structure Determination

A least-squares refinement of atomic parameters directly referred to those of Ag- β -alumina gave an unsatisfactory R value ($R > 0.60$), where R is given by $[\sum |F_o| - |F_c|] / \sum |F_o|$, after 5 cycles of the refinement. Therefore, the refinement was started from a three-dimensional Patterson synthesis. However, it was clarified at the stage of the refinement at which there was no difference in the packing arrangement of the component atoms among Na-, Ag-, and TI- β -alumina compounds. One kind of thallium atom, located around the position $(\frac{2}{3} \frac{1}{3} \frac{1}{4})$ with the Wyckoff

notation (*h*) and with the probability of the site being occupied, 0.5; the atoms of the spinel block obtained from the Patterson synthesis were included into the structure factor calculation by assigning the same isotropic temperature factor of 2.0 to all the atoms. The *R* factor was 0.44. Other kinds of thallium atom could be found by calculating the Fourier synthesis using the parameters of *R* = 0.44. The thallium species located at the position (000) with the Wyckoff notation (*a*) and another located near the position (000) between the two kinds of the thallium atom previously described were added into a block-diagonal least-squares refinement. Through-

out the refinement, occupation parameters were fixed and position and thermal parameters were refined with small damping factors. An *R* value of 0.24 was obtained after 5 cycles of the refinement. The thallium species located at the position ($\frac{2}{3} \frac{1}{3} \frac{1}{4}$) was added for the convenience of the refinement and the atomic parameters were refined with anisotropic temperature factors for all the atoms. The occupation parameters of the thallium atom were adjusted by integrating the electron density of the Fourier synthesis at each stage of the refinement. At the stage, *R* \leq 0.10, occupation parameters were varied step by step with a change of 0.001 to improve the *R*

TABLE I
FINAL ATOMIC COORDINATES ($\times 10^4$) AND THERMAL PARAMETERS ($\times 10^4$)^a

Atom	I	II	III	IV	<i>x</i>	<i>y</i>	<i>z</i>	β_{11}	β_{22}	β_{33}	β_{12}	β_{13}	β_{23}
Tl(1)	2	<i>d</i>	$\bar{6}m2$	0.540	6667 (0)	3333 (0)	2500 (0)	2279 (222)	9116 (888)	58 (8)	4558 (444)	0 (0)	0 (0)
Tl(1')	6	<i>h</i>	<i>mm</i>	1.320	6688 (25)	3376 (13)	2500 (0)	1778 (72)	7113 (288)	28 (3)	3556 (144)	0 (0)	0 (0)
Tl(2)	2	<i>b</i>	$\bar{6}m2$	0.072	0 (0)	0 (0)	2500 (0)	1467 (1162)	5867 (4648)	15 (44)	2934 (2324)	0 (0)	0 (0)
Tl(2')	6	<i>h</i>	<i>mm</i>	0.732	9233 (16)	8465 (15)	2500 (0)	2356 (236)	9426 (944)	32 (7)	4713 (472)	0 (0)	0 (0)
Al(1)	12	<i>k</i>	<i>m</i>	12	8323 (9)	6647 (7)	1042 (1)	181 (38)	726 (152)	13 (4)	363 (76)	-5 (13)	-10 (26)
Al(2)	4	<i>f</i>	<i>3m</i>	4	3333 (0)	6667 (0)	244 (3)	291 (106)	1164 (424)	3 (8)	582 (212)	0 (0)	0 (0)
Al(3)	4	<i>f</i>	<i>3m</i>	4	3333 (0)	6667 (0)	1750 (3)	417 (113)	1666 (452)	-23 (7)	833 (226)	0 (0)	0 (0)
Al(4)	2	<i>a</i>	$\bar{3}m$	2	0 (0)	0 (0)	0 (0)	510 (212)	2040 (848)	17 (14)	1020 (424)	0 (0)	0 (0)
O(1)	12	<i>k</i>	<i>m</i>	12	1581 (20)	3162 (40)	489 (3)	249 (116)	997 (464)	11 (8)	499 (232)	9 (25)	18 (51)
O(2)	12	<i>k</i>	<i>m</i>	12	5015 (19)	30 (0)	1445 (3)	92 (77)	368 (308)	16 (10)	184 (154)	15 (23)	29 (46)
O(3)	4	<i>f</i>	<i>3m</i>	4	6667 (0)	3333 (0)	547 (6)	300 (242)	1199 (968)	1 (16)	600 (484)	0 (0)	0 (0)
O(4)	4	<i>e</i>	<i>3m</i>	4	0 (0)	0 (0)	1401 (7)	582 (287)	2326 (1148)	-37 (18)	1163 (574)	0 (0)	0 (0)
O(5)	2	<i>c</i>	$\bar{6}m2$	2	3333 (0)	6667 (0)	2500 (0)	1938 (769)	7751 (3076)	-83 (24)	3876 (1538)	0 (0)	0 (0)

^a I, number of positions; II, Wyckoff notation, III, point symmetry; IV, number of atom per unit cell. Estimated standard deviations are shown in parentheses. The *y* fraction is related to the *x* fraction with the equation $y = 2x$. Thermal parameters are in the form $\exp[-(h^2\beta_{11} + k^2\beta_{22} + l^2\beta_{33} + 2hk\beta_{12} + 2hl\beta_{13} + 2kl\beta_{23})]$. $\beta_{22} = 4\beta_{11}$. $\beta_{12} = 2\beta_{11}$. $\beta_{23} = 2\beta_{13}$.

TABLE II
OBSERVED AND CALCULATED STRUCTURE FACTORS

<i>h</i>	<i>k</i>	<i>l</i>	F_o	F_c	<i>h</i>	<i>k</i>	<i>l</i>	F_o	F_c	<i>h</i>	<i>k</i>	<i>l</i>	F_o	F_c	<i>h</i>	<i>k</i>	<i>l</i>	F_o	F_c
1	0	0	9.2	11.7	4	1	4	46.3	42.7	2	0	9	50.1	48.1	2	1	13	21.2	20.6
1	1	0	99.2	104.1	5	0	4	18.3	18.6	2	1	9	23.4	22.8	4	0	13	27.4	22.5
2	0	0	34.2	34.4	5	2	4	28.1	30.3	3	0	9	7.4	8.5	4	2	13	31.4	28.3
2	1	0	23.3	23.5	6	3	4	14.0	20.4	3	1	9	7.5	6.8	6	2	13	19.6	14.8
2	2	0	150.1	165.2	7	1	4	16.2	15.4	3	2	9	12.2	13.6	6	4	13	15.8	14.0
3	0	0	67.6	61.3	1	0	5	48.5	49.7	4	0	9	41.2	40.6	8	0	13	17.4	15.8
3	1	0	16.4	18.5	2	0	5	76.9	74.0	4	2	9	20.0	18.8	0	0	14	118.9	115.3
3	3	0	40.0	42.2	2	1	5	36.8	37.1	0	0	10	115.9	110.1	1	0	14	17.1	18.5
4	0	0	31.1	31.3	3	1	5	18.9	17.7	1	0	10	25.6	26.0	1	1	14	54.0	54.3
4	1	0	41.0	37.8	3	2	5	22.7	22.5	1	1	10	70.2	69.5	2	0	14	83.1	81.0
4	2	0	16.0	17.7	4	0	5	54.5	52.8	2	0	10	13.5	11.1	2	1	14	25.5	24.4
4	4	0	68.4	73.1	4	2	5	27.7	26.2	2	1	10	37.4	35.1	2	2	14	64.3	62.4
5	0	0	15.4	16.9	6	2	5	15.8	20.3	2	2	10	33.4	33.5	3	0	14	33.0	32.1
5	2	0	24.4	20.2	0	0	6	81.9	87.7	3	0	10	43.2	42.9	3	1	14	23.3	21.7
6	0	0	81.1	78.0	1	1	6	27.6	26.4	3	1	10	28.8	26.8	3	2	14	13.1	12.3
7	1	0	14.3	15.0	2	0	6	65.1	63.1	3	2	10	15.4	16.1	3	3	14	19.6	24.3
1	0	1	42.8	47.5	2	1	6	11.0	9.4	3	3	10	27.4	28.4	4	0	14	61.7	60.4
2	1	1	35.0	34.5	2	2	6	28.9	31.9	4	0	10	7.5	3.7	4	1	14	19.2	19.5
3	1	1	16.5	14.3	4	0	6	42.0	42.6	4	1	10	26.7	25.6	4	2	14	42.8	41.6
3	2	1	22.1	22.8	4	2	6	24.6	26.1	4	3	10	11.6	13.1	4	4	14	26.5	30.0
0	0	2	37.4	36.9	6	2	6	15.8	18.4	5	0	10	27.3	27.3	5	0	14	18.3	16.1
1	0	2	26.2	26.7	8	0	6	13.8	15.9	5	1	10	15.4	18.5	5	2	14	11.2	11.7
1	1	2	62.1	62.9	1	0	7	90.3	96.0	5	2	10	15.9	17.3	6	0	14	28.8	26.9
2	0	2	11.9	7.8	2	0	7	10.8	8.2	7	2	10	11.6	14.0	6	2	14	26.5	29.2
2	1	2	25.9	25.5	2	1	7	77.6	77.8	1	0	11	44.7	43.1	6	4	14	20.5	20.7
3	0	2	33.9	34.7	3	0	7	12.4	12.1	2	0	11	78.1	76.0	8	0	14	26.5	24.9
3	1	2	24.5	23.8	3	1	7	49.6	47.1	2	1	11	35.7	33.9	10	0	14	16.8	16.2
3	2	2	15.7	18.0	3	2	7	49.7	50.3	3	0	11	10.4	10.3	1	0	15	44.4	43.6
3	3	2	19.1	19.4	4	3	7	28.8	34.3	3	1	11	16.5	16.0	2	0	15	34.4	33.8
4	1	2	15.1	16.8	5	0	7	37.9	37.8	3	2	11	21.3	20.4	2	1	15	38.2	35.0
5	0	2	14.3	17.0	5	1	7	34.5	34.9	4	0	11	63.5	61.7	3	1	15	21.1	18.9
6	1	2	13.5	12.3	5	3	7	19.3	17.1	4	2	11	35.0	35.5	3	2	15	24.4	23.9
1	0	3	38.2	39.1	6	1	7	23.1	22.1	4	3	11	9.2	11.9	4	0	15	30.2	29.6
2	0	3	47.9	52.1	7	0	7	18.6	22.5	5	0	11	10.6	7.2	4	1	15	6.0	7.9
2	1	3	34.1	33.3	7	2	7	13.9	19.0	6	2	11	20.5	26.6	4	2	15	13.2	12.5
3	0	3	15.1	14.9	0	0	8	111.4	115.7	8	0	11	17.7	19.6	5	0	15	12.8	10.3
3	1	3	10.8	9.9	1	0	8	10.9	6.9	0	0	12	68.1	66.2	5	1	15	14.9	17.1
3	2	3	15.2	14.9	1	1	8	61.7	59.2	1	0	12	10.2	12.1	5	4	15	7.6	11.6
4	0	3	49.7	50.8	2	0	8	23.3	16.4	1	1	12	76.0	75.0	6	1	15	11.2	9.7
4	2	3	26.6	26.3	2	2	8	50.5	51.9	2	1	12	13.5	15.4	0	0	16	56.3	52.9
0	0	4	38.4	38.0	3	0	8	36.7	32.7	2	2	12	27.6	27.0	1	1	16	66.3	64.8
1	0	4	13.2	15.5	3	3	8	19.8	20.5	3	0	12	50.5	49.8	2	2	16	17.6	15.6
1	1	4	100.9	104.8	4	0	8	9.5	2.3	3	1	12	15.7	15.4	3	0	16	43.5	43.2
2	0	4	42.1	36.3	4	1	8	20.8	16.7	3	3	12	30.3	30.4	3	3	16	29.0	28.0
2	1	4	25.0	24.4	4	2	8	11.9	5.9	4	0	12	11.4	9.8	4	1	16	28.5	26.7
3	0	4	69.5	69.1	4	4	8	20.0	26.4	4	1	12	32.2	29.8	5	2	16	15.9	19.4
3	1	4	19.6	19.0	5	2	8	12.0	10.9	5	2	12	18.9	21.2	1	0	17	22.1	21.6
3	3	4	44.0	42.1	6	0	8	22.3	20.2	1	0	13	22.3	23.8	2	0	17	39.7	38.8
4	0	4	20.5	21.0	1	0	9	29.1	30.2	2	0	13	50.2	43.2	2	1	17	21.4	19.7

TABLE II (continued)

<i>h</i>	<i>k</i>	<i>l</i>	F_0	F_c	<i>h</i>	<i>k</i>	<i>l</i>	F_0	F_c	<i>h</i>	<i>k</i>	<i>l</i>	F_0	F_c	<i>h</i>	<i>k</i>	<i>l</i>	F_0	F_c
3	0	17	11.7	10.8	3	2	21	30.5	33.1	1	1	26	49.1	50.6	1	1	32	31.8	31.0
4	0	17	37.7	36.7	4	0	21	15.8	13.6	2	0	26	26.1	25.0	3	0	32	18.5	21.6
4	2	17	18.3	18.2	4	3	21	18.5	20.5	2	1	26	18.9	19.3	3	3	32	15.9	14.1
0	0	18	38.0	37.9	5	0	21	20.6	20.2	2	2	26	43.2	43.7	4	1	32	16.3	13.6
1	0	18	19.8	18.8	5	1	21	19.9	22.5	3	0	26	34.3	36.3	1	0	33	28.9	31.6
1	1	18	56.9	54.9	5	3	21	13.6	12.5	3	1	26	15.0	17.5	2	1	33	28.0	28.6
2	0	18	18.8	17.1	6	1	21	16.3	15.9	3	2	26	24.3	26.6	3	1	33	17.2	17.6
2	1	18	23.9	22.7	0	0	22	40.7	40.5	4	0	26	19.6	22.1	3	2	33	18.0	19.9
2	2	18	8.9	8.0	1	0	22	15.6	17.0	4	1	26	24.6	25.2	4	0	33	14.5	12.1
3	0	18	37.1	37.0	1	1	22	39.8	38.6	5	0	26	14.8	15.0	5	0	33	19.2	15.4
3	1	18	22.8	20.5	2	0	22	24.8	25.3	6	0	26	23.6	22.2	0	0	35	32.6	34.6
3	2	18	14.5	16.0	2	1	22	19.9	18.6	1	0	27	17.3	18.4	2	0	34	20.1	21.5
3	3	18	23.7	23.2	2	2	22	14.0	13.1	2	0	27	26.8	24.7	2	2	34	17.8	16.0
4	1	18	24.5	22.4	3	0	22	25.8	24.2	2	1	27	17.0	16.6	4	0	34	16.8	20.3
4	2	18	16.1	12.6	3	1	22	20.9	19.0	4	0	27	17.4	15.3	1	0	35	17.9	19.8
5	0	18	16.3	17.8	3	2	22	16.6	15.4	4	2	27	24.5	20.6	2	1	35	15.8	17.1
5	2	18	13.1	17.2	3	3	22	14.5	16.6	0	0	28	79.3	76.2	4	1	35	14.2	14.8
6	1	18	13.3	11.8	4	0	22	21.8	22.3	1	1	28	31.8	32.9	0	0	36	44.6	45.9
1	0	19	43.6	44.5	4	1	22	14.6	14.2	2	2	28	48.3	46.9	1	1	36	33.6	33.9
2	0	19	37.8	35.2	4	2	22	14.0	14.1	3	0	28	21.6	21.1	2	2	36	25.8	27.9
2	1	19	37.4	36.8	5	0	22	12.9	12.7	3	3	28	13.1	15.4	3	0	36	26.1	25.1
3	0	19	6.5	6.7	1	0	23	19.0	19.5	4	1	28	14.6	13.1	1	0	37	14.1	16.2
3	1	19	23.2	21.7	2	0	23	23.5	22.5	6	0	28	24.6	25.5	2	0	37	15.5	17.4
3	2	19	26.5	25.8	4	0	23	23.2	22.7	1	0	29	24.3	24.2	1	1	38	22.3	20.9
4	0	19	32.9	32.1	2	1	23	19.2	17.1	2	0	29	20.3	19.0	0	0	40	51.4	54.1
4	2	19	15.9	15.2	0	0	24	16.5	10.5	2	1	29	20.3	19.3	1	1	40	24.0	26.8
5	1	19	16.1	18.3	1	1	24	44.3	45.1	4	0	29	16.0	18.9	2	0	40	16.1	16.9
0	0	20	106.3	107.4	3	0	24	31.9	31.0	0	0	30	37.6	38.0	1	0	41	15.7	14.9
1	0	20	18.5	15.2	3	3	24	22.4	21.2	1	0	30	12.0	12.6	0	0	42	16.7	15.7
1	1	20	16.3	15.4	4	1	24	20.4	19.8	1	1	30	29.9	29.9	1	1	42	14.6	14.9
2	2	20	59.1	60.4	4	4	24	14.0	7.2	2	1	30	18.7	17.9	0	0	44	16.4	15.9
4	0	20	8.5	8.1	6	0	24	16.0	15.9	2	2	30	15.0	17.9	1	1	44	21.0	23.6
4	4	20	30.5	35.3	1	0	25	19.0	19.9	3	0	30	17.7	19.2	2	0	45	22.7	22.1
6	0	20	31.9	31.4	2	0	25	43.0	43.5	3	1	30	15.1	15.4	4	0	45	20.0	21.4
8	2	20	16.1	18.7	2	1	25	17.0	16.5	3	3	30	13.2	14.7	0	0	46	17.3	17.4
1	0	21	52.4	53.3	4	0	25	40.8	38.8	5	0	30	15.6	16.1	1	0	47	19.9	20.3
2	0	21	14.1	10.8	4	2	25	25.2	23.5	1	0	30	13.6	13.5	2	1	47	15.6	19.3
2	1	21	44.7	44.3	0	0	26	77.0	74.4	2	0	31	31.9	31.8					
3	1	21	29.8	28.5	1	0	26	13.2	15.0	4	0	31	28.2	29.9					

value. An R value of 0.063 was so obtained. The occupation parameters are shown in Table I. Tl- β -alumina was found to have the composition $\text{Tl}_{2.66}\text{Al}_{22}\text{O}_{34}$ from the occupation parameters. The chemical analysis of Tl- β -alumina was not carried out. However, it may be suggested from the comparison of the observed value of the crystal density and the calculated one that the number of the

thallium atom involved in a unit cell is somewhat smaller than that estimated from the occupation parameters, and this might be true because the correlation between occupation and thermal parameters can easily be considered at this stage of the refinement. This also may be said in comparison with the composition of Ag- and Na- β -alumina; $\text{Ag}_{2.4}\text{Al}_{22}\text{O}_{34.2}$ estimated from the occupation

parameters and $\text{Na}_{2.58}\text{Al}_{21.81}\text{O}_{34}$ estimated from the occupation parameters with a good agreement of the composition $\text{Na}_{2.55}\text{Al}_{21.82}\text{O}_{34}$ observed by neutron activation analysis.

The reflection data corrected by representing the crystal as a sphere of equivalent volume with $l = 0.02$ mm was calculated and was compared at the later stage of the refinement with the reflection data without the absorption correction. However, the reflection data without the absorption correction gave a better agreement between the observed values of the structure factor and the calculated values, and moreover, showed smaller anisotropic temperature factors, B_{33} , of the Al(3), O(4) and O(5) atoms in the negative direction. Therefore, the reflection data without the absorption correction was used for the discussion. This indicates that the absorption correction by representing the crystal used as a sphere of equivalent volume is insufficient or absorption may be compensating with extinction. The negative values for the diagonal terms of the anisotropic temperature factors were unusual, but were also reported for Ag- β -alumina.

The final atomic and thermal parameters are listed in Table I. A complete list of the observed and calculated structure factors is shown in Table II. Atomic scattering curves taken from the International Tables for X-ray Crystallography were used throughout.

Description and Discussion of the Crystal Structure

Lattice constants of related β -alumina compounds are $a = 5.595$, $c = 22.488$ Å for Ag- β -alumina; and $a = 5.594$, $c = 22.53$ Å for Na- β -alumina. The length of a repetition unit along the c -axis was found to be sensitive to the size of the mobile ion, but no significant deviations among the length of a repetition unit along the a -axis were observed within standard deviations. Therefore, a different property between the binding within and between the layers can be suggested. A unit lattice of Tl- β -alumina observed by the authors is somewhat longer along the c -axis than that of Tl- β -alumina reported by Yao and Kummer (17).

A perspective drawing of the crystal structure is shown in Fig. 2. The Tl^+ ions are situated between large blocks of the spinel structure and the two successive spinel blocks are covalently bonded by the corner-sharing $\text{O}_3\text{Al-O-AlO}_3$ tetrahedra along the c -axis. The mirror plane is located on the conduction plane and contains a common oxygen of the $\text{O}_3\text{Al-O-AlO}_3$ spacer column. The space necessary for the movement of the thallium ion is preserved by the column. In the spinel block, the O^{2-} ions are arranged in cubic-packing and the aluminium atoms are located in the octahedral and the tetrahedral holes. The aluminium layer located near the conduction plane consists of one kind of aluminium ions with the octahedral coordination and is considered to be more ionized than the other because the aluminium ion with the octahedral coordination is thought to be more polarized than that with the tetrahedral. The aluminium layer located halfway between successive conduction planes consists of two kinds of the aluminium ions with the octahedral and the tetrahedral coordinations.

Tl- β -alumina has a unit lattice which is longer by 0.47 and 0.43 Å along the c -axis than that of Ag- and Na- β -alumina. The volume of the spinel block is almost equal for these compounds, but the covalently bonded $\text{O}_3\text{Al-O-AlO}_3$ column makes a remarkable contribution to the variation of the length of a unit lattice along the c -axis according to the species of the mobile ion. Going into details, about one-half of the elongation is brought out by the elongation of the bond length between the O(5) located (on the conduction layer) and Al(3) atoms, and the other half of the elongation by expanding the O(2)-Al(3)-O(5) angle while keeping the O(2)-Al(3) bond lengths constant. The observed values of the Al(3)-O(5) bond length found for Ag- and Na- β -alumina are 1.675 and 1.677 Å, respectively, and these are unusual ones. For Tl- β -alumina, the corresponding value observed was 1.72 Å and is comparable to a usual one for an aluminium-oxygen bond length. The extreme contraction along the c -axis of the aluminium tetrahedra in the column is thus lengthened in Tl- β -alumina.

Bond lengths and angles are listed in Table III and are shown in Fig. 3. No significant deviations of bond lengths were observed in the spinel block from those of Ag- and Na- β -alumina. In the column, four Al-O bond lengths were observed to be shorter altogether in comparison with the ordinary Al-O bond length. In the octahedra in which the Al(1) atom is located as a center, three aluminium-oxygen bond lengths located near the conduction plane are shorter than the other. In the tetrahedra in which the Al(2) atom is located as a center, the aluminium-oxygen bond length lengthened parallel to the c -axis is longer than the other.

The occupation percentages of the mobile ion in the conduction layer is shown in Fig. 4 for Tl-, Ag-, and Na- β -alumina. The mobile ion moves between the successive BR positions

by way of the aBR position. The BR position surrounded by six oxygens has the highest occupancy percentage throughout all of the β -alumina compounds. The thallium ion has about 70% occupancy for the BR position. The electron density at the conduction plane is shown in Fig. 5. A stabilized position, Tl(2'), in potential energy (this is called hereafter as aBR' position) was found to exist as an introductory position to the aBR position. Although the Tl(1) position is located at the center of six O(2) atoms, the Tl(2) position is located between two O(4) atoms which are located just above and below it. The Tl(2)-O(4) distance observed is $2.52 \pm 0.02 \text{ \AA}$, which is much shorter than the Tl(1)-O(2) distance ($2.90 \pm 0.01 \text{ \AA}$). The Tl(2') atom is located $0.74 \pm 0.01 \text{ \AA}$ apart from the Tl(2) atom and the Tl(2')-O(4) distance observed is somewhat

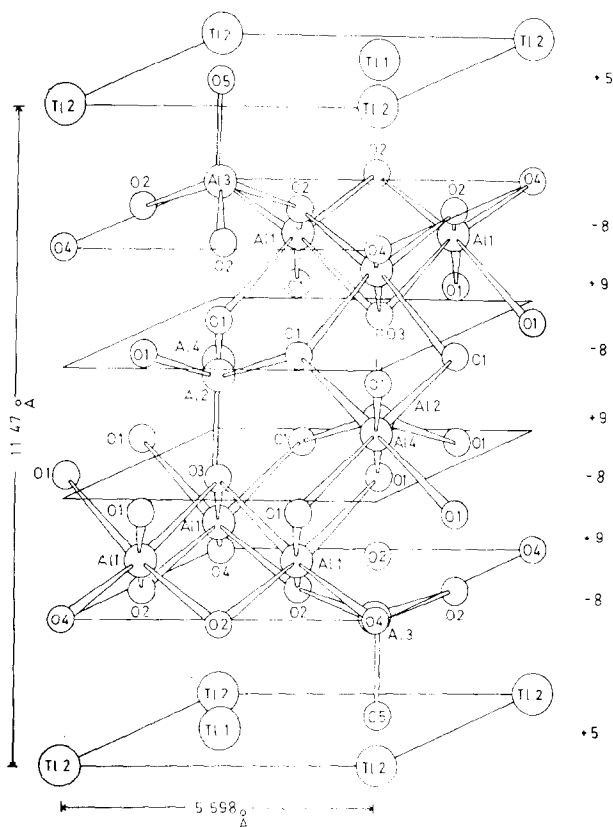


FIG. 2. A perspective drawing of the crystal structure to the c -axis. The estimated electric charges of each packing layer per unit cell are described on the right-hand side of each packing layer.

TABLE III
BOND LENGTHS AND ANGLES OF Tl-, Ag-, AND Na- β -ALUMINA^a

	Number of bonds	Tl- β -alumina	Ag- β -alumina	Na- β -alumina (Felsche (20))	Na- β -alumina (Peters <i>et al.</i> (18))
Bond lengths					
Octahedral coordination					
Al(1)-O(1)	2	2.026 \pm 0.012 Å	2.017 Å	2.026 Å	2.022 Å
Al(1)-O(2)	2	1.852 \pm 0.010	1.839	1.841	1.837
Al(1)-O(3)	1	1.966 \pm 0.009	1.973	1.947	1.970
Al(1)-O(4)	1	1.822 \pm 0.008	1.821	1.818	1.819
Al(4)-O(1)	6	1.899 \pm 0.012	1.893	1.885	1.895
Tetrahedral coordination					
Al(2)-O(1)	3	1.790 \pm 0.009	1.806	1.798	1.801
Al(2)-O(3)	1	1.814 \pm 0.015	1.800	1.777	1.809
Al(3)-O(2)	3	1.774 \pm 0.009	1.762	1.758	1.768
Al(3)-O(5)	1	1.720 \pm 0.006	1.675	1.685	1.677
Bond angles					
Octahedral coordination					
O(1)-Al(1)-O(2)		90.4 \pm 0.3	90.70	90.45°	
O(1)-Al(1)-O(3)		89.2 \pm 0.3	89.19	88.55	
O(1)-Al(1)-O(4)		84.5 \pm 0.3	84.04	84.18	
O(2)-Al(1)-O(3)		86.2 \pm 0.4	86.09	86.41	
O(1)-Al(4)-O(1')		88.7 \pm 0.3	92.06	91.41	
O(1)-Al(4)-O(1'')		91.3 \pm 0.3	92.06	91.41	
Tetrahedral coordination					
O(1)-Al(2)-O(1')		110.6 \pm 0.4	110.37	110.93	
O(1)-Al(2)-O(3)		108.3 \pm 0.3	108.56	107.96	
O(2)-Al(3)-O(2')		105.5 \pm 0.5	107.55	107.03	
O(2)-Al(3)-O(5)		113.2 \pm 0.3	111.33	111.82	

^a O(1)-Al(4)-O(1') expresses an angle made by two oxygens of the same layer and the aluminium. O(1)-Al(4)-O(1'') expresses an angle made by two oxygens of the different layers with each other and the aluminium.

lengthened to 2.63 \pm 0.02 Å. A steric repulsion between the Tl(2') and the O(4) atoms is then relieved. In related β -alumina compounds, the O(4) atom is found to be somewhat more deviated from the conduction layer than the O(2) atoms; 0.10, 0.095, and 0.095 Å is observed in Tl-, Ag-, and Na- β -alumina, respectively.

In Tl- β -alumina, the *aBR'* and the *aBR* positions appeared in marked relief in the Fourier synthesis. In Na- β -alumina, the *aBR'* position was also found, however, that the sodium ion has no occupancy at the *aBR* position. In Ag- β -alumina, both positions are occupied by silver ion, but the *aBR'* position is

very much smeared in the Fourier synthesis. Because the *aBR* position is stabilized by the covalent bonding character and the *aBR'* position appeared to be due to the strong ionic character or the steric repulsion of ions, the thallium ion is considered to have some occupancy at the *aBR* and the *aBR'* positions due to its slightly covalent character and its steric largeness.

The electric charges distributed for each packing layer were roughly estimated by assigning +3, +1, and -2 for the aluminium, thallium, and oxygen atoms, respectively. The Al-O-Al atoms in the covalent column were included in the conduction layer. The calcu-

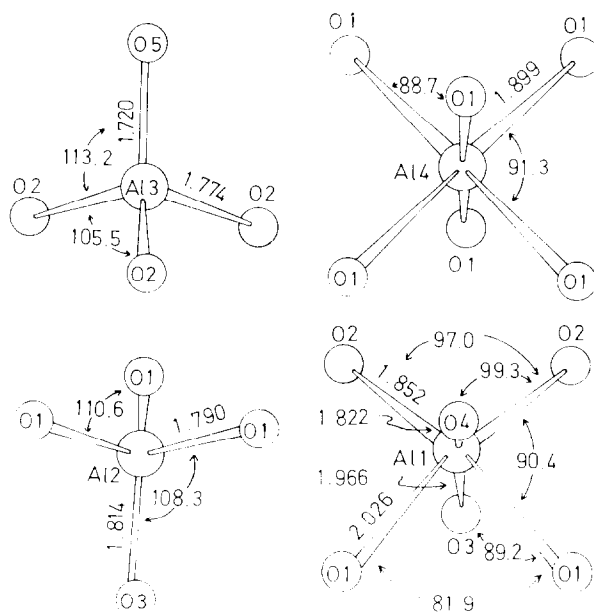


FIG. 3. Bond lengths and angles of the six-coordination and the four-coordination groups around the aluminium atom. The perspective direction is identical with that of Fig. 2.

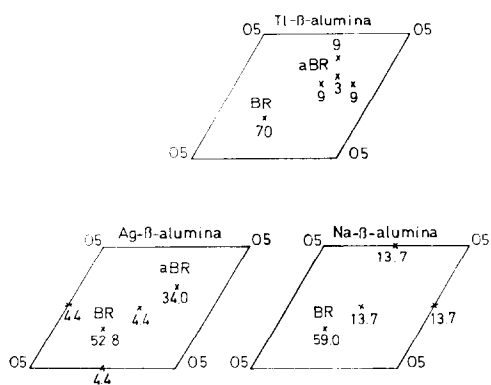


FIG. 4. The occupational percentages of the mobile ion in the conduction plane. BR and aBR positions are shown in this figure.

lated electric charges of each packing layer per unit cell are described on the right-hand side of each packing layer in Fig. 2. It is interesting that the conduction layer is less positively charged in comparison with the aluminium layer and the positively charged mobile ion hops between available sites so as to homogenize the distribution of the positive charge. Nonstoichiometric β -alumina compounds

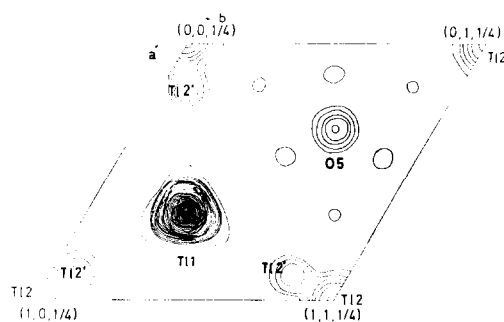


FIG. 5. The electron density in the conduction plane with arbitrary interval.

show the concentration of the mobile ion species as being a little larger than that of the general formula, $M_2O \cdot 11Al_2O_3$, and that of the aluminium species being a little smaller. It is interesting that the tendency toward insufficiency of the positive charge in the conduction layer is diminished by an increase of the amount of the mobile ion consists in the nonstoichiometric phenomena found in β -alumina compounds.

The extraordinarily large anisotropic vibrations of the atoms in the conduction plane

were also observed as in the case of Ag- and Na- β -alumina.

Calculations were carried out on a HITAC 8700 computer at the Computer Center of the University using the Universal Crystallographic Computation Program System.

Acknowledgment

The authors wish to express their sincere thanks to Professor Yoshihiko Saito for his kindness and for the use of the diffractometer of his laboratory and his helpful discussions.

References

1. J. HLADIK (Ed.), "Physics of Electrolytes," Vol. II, Part 24, Academic Press, London/New York (1972).
2. M. W. BREITER, "Electrochemical Processes in Fuel Cells," Springer-Verlag, Berlin (1969).
3. T. TAKAHASHI, *Denki Kagaku* **36**, 481 (1968).
4. H. IKEDA, K. TADA, Y. IKUKAWA, AND Y. OE, *Sanyo Tech. Rev.* **4**, No. 2, 3 (1972).
5. N. ISHIBASHI, *Japan Analyst* **20**, 749 (1971).
6. J. J. LINGANE, *Anal. Chem.* **39**, 881 (1967).
7. N. T. CROSBY, A. L. DENNIS, AND J. G. STEVENS, *Analyst* **93**, 643 (1968).
8. M. J. RICE AND W. L. ROTH, *J. Solid State Chem.* **4**, 294 (1972).
9. R. W. SCHMITT, *Phys. Today* **24**, 44 (1971).
10. L. HEYNE, *Electrochimica Acta* **15**, 1251 (1970).
11. J. KUMMER AND M. E. MILBERG, *Chem. Eng. News* **47** (20), 90 (1969).
12. L. W. STROCK, *Z. Physik. Chem.* **B25**, 441 (1934).
13. S. GELLER, *Science* **157**, 310 (1967).
14. J. A. KETELAAR, *Trans. Faraday Soc.* **34**, 874 (1934).
15. M. S. WHITTINGHAM AND R. A. HUGGINS, *J. Electrochem. Soc.* **118**, 1 (1971).
16. M. S. WHITTINGHAM AND R. A. HUGGINS, *J. Chem. Phys.* **54**, 44 (1971).
17. Y. Y. YAO AND J. T. KUMMER, *J. Inorg. Nucl. Chem.* **29**, 2453 (1967).
18. C. R. PETERS, M. BETTMAN, J. W. MOORE, AND M. D. GLICK, *Acta Crystallogr.* **B27**, 1826 (1971).
19. W. L. ROTH, *J. Solid State Chem.* **4**, 60 (1972).
20. J. FELSCH, *Naturwissenschaften* **54**, 612 (1967).